Journal of the Korean Chemical Society
2016, *Vol. 60, No. 3*
Printed in the Republic of Korea
http://dx.doi.org/10.5012/jkcs.2016.60.3.194

New Low–Band Gap 2D-Conjugated Polymer with Alkylthiobithiophene-Substituted Benzodithiophene for Organic Photovoltaic Cells

Eun Hye Park, Jong Jun Ahn, Hee Su Kim, Ji-Hoon Kim, and Do-Hoon Hwang*
Department of Chemistry and Chemistry Institute for Functional Materials, Pusan National University, Busan 46241, Korea.
**E-mail: do-hoonhwang@pusan.ac.kr*
(Received April 1, 2016; Accepted April 26, 2016)

ABSTRACT. Two conjugated semiconducting copolymers consisting of 4,7-bis(4-(2-ethylhexyl)-2-thiophene)-2,1,3-benzothiadiazole (DTBT) and benzo[1,2-b:4,5-b']dithiophene with 5-(2-ethylhexyl)-2,2'-bithiophene (BDTBT) or 5-(2-ethylhexylthio)-2,2'-bithiophene (BDTBT-S) were designed and synthesized as donor materials for organic photovoltaic cells (OPVs). Alkylthio-substituted PBDTBT-S-DTBT showed a higher hole mobility and lower highest occupied molecular orbital (HOMO) energy level (by 0.08 eV) than the corresponding alkyl-substituted PBDTBT-DTBT. An OPV fabricated using PBDTBT-S-DTBT showed higher V_{OC} and J_{SC} values of 0.83 V and 7.56 mA/cm^2, respectively, than those of a device fabricated using PBDTBT-DTBT (0.74 V) leading to a power conversion efficiency of 2.05% under AM 1.5G 100 mW/cm^2 illumination.

Key words: Organic photovoltaic cell, Organic thin-film transistor, Power conversion efficiency, Benzodithiophene

INTRODUCTION

Organic photovoltaic cells (OPVs) are remarkable clean and renewable energy sources that help reduce fossil-fuel depletion and the corresponding environmental problems. OPVs also have many advantages over silicon-based inorganic solar cells such as their light weight, flexibility, and processability.[1] To increase the power conversion efficiency (PCE) of OPVs, significant efforts have been made to design and synthesize new conjugated semiconducting polymers.[2–4] These include the application of donor–acceptor (D–A)–type copolymers to reduce the band-gap energies of semiconducting donor polymers. The donor and acceptor units in the copolymer affect the highest occupied molecular orbital (HOMO) and lowest unoccupied molecular orbital (LUMO) energy levels and induce intramolecular charge transfer (ICT).[5] To control the HOMO and LUMO frontier orbital energy levels, structural modifications involving the introduction of heteroatoms, such as fluorine, have attracted significant research interest.[6–10] The introduction of fluorine atoms could effectively lower the HOMO energy levels of donor polymers, which would increase the V_{OC} values of the fabricated OPVs because they are proportional to the energy gap between the HOMO of the donor polymer and LUMO of the fullerene-based acceptor.[6,7,11] Benzo[1,2-b:4,5-b']dithiophene (BDT) is a popular donor building block for D–A copolymers.[12–14] Recently, *Lee et al.* introduced dialkylthio side chains on BDT for tuning the optoelectronic properties of D-A copolymers and found that the polymers with the dialkylthio side chain possessed a down-shifted HOMO energy level compared to that of corresponding polymer with a dialkoxy side chain.[15] The d-orbital of the sulfur atom could accept π-electrons from the p-orbital of the adjacent aromatic group; therefore, the alkylthio substituent could affect the energy levels of the HOMO/LUMO frontier orbitals. Accordingly, the π-acceptor capability of the sulfur atom reduces the HOMO energy levels, which improves the PCEs of the OPVs because of the resultant higher V_{OC} values. Li *et al.* synthesized two-dimensional (2D) conjugated polymers containing an alkylthiothiophene-substituted BDT building block and reported that the HOMO energy levels of the polymers decreased.[15]

In this study, we designed and synthesized a new BDT derivative containing alkylthio-substituted bithiophene (BDTBT-S) as a new donor building block for D–A–type low–band gap copolymers for OPVs, as shown in *Scheme* 1. The alkylthio-substituted bithienyl group was introduced into BDT in order to tune the HOMO energy level, as mentioned above, and also extend the conjugation length of the resulting 2D-conjugated polymer for enhanced light absorption. The synthesized BDTBT-S was copolymerized with alkylthiophene-substituted benzothiadiazole (DTBT) to give a copolymer, i.e., PBDTBT-S-DTBT. We also synthesized a corresponding alkyl-substituted copolymer, PBDTBT-DTBT, which is also a new polymer, for comparison of its optical and electrical properties with those of PBDTBT-S-DTBT. Poly{4,8-bis((2-ethylhexylthio)-2,2'-bithiophene)benzo[1,2-b:4,5-b']dithiophene-alt-4,7-bis(4-(2-ethylhexyl)-2-thio-

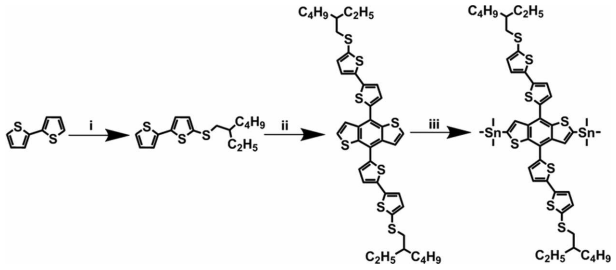

***Scheme* 1.** Synthetic routes to the monomers: (i) n-BuLi, sulfur powder, 2-ethylhexylbromide, THF, 0 °C then 20 °C, (ii) n-BuLi, benzo[1,2-b:4,5-b′]dithiophene-4,8-dione, $SnCl_2 \cdot 2H_2O$, THF, 0 °C then 50 °C, and (iii) TMEDA, n-BuLi, $Sn(Me)_3Cl$, THF, −78 °C then 20 °C.

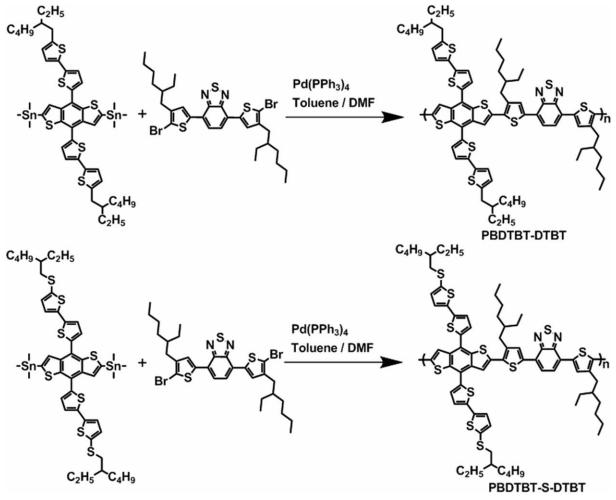

***Scheme* 2.** Syntheses of PBDTBT-DTBT and PBDTBT-S-DTBT polymers.

phene)-2,1,3-benzothiadiazole} (PBDTBT-S-DTBT) and poly{4,8-bis((2-ethylhexyl)-2,2'-bithiophene)benzo[1,2-b:4,5-b′]dithiophene-alt-4,7-bis(4-(2-ethylhexyl)-2-thiophene)-2,1,3-benzothiadiazole} (PBDTBT-DTBT) were synthesized via Stille cross-coupling, as shown in *Scheme* 2.

EXPERIMENTAL

Materials

2,2'-Bithiophene, n-butyllithium (1.6 M), 2-ethylhexyl bromide, and trimethyltin chloride (1.0 M) were purchased from Aldrich. Sulfur was purchased from Dae Jung, and tetrakis(triphenylphosphine)palladium(0) was purchased from Strem. [6,6]-Phenyl C_{71}-butyric acid methyl ester ($PC_{71}BM$) was purchased from EM-index. All materials were used without further purification. THF solvent was dried and purified by fractional distillation over sodium/benzophenone and handled in a moisture-free atmosphere. 4,7-Bis(5-bromo-4-(2-ethylhexyl)thiophen-2-yl)-2,1,3-benzothiadiazole[1,3] and 2,6-bis(trimethyltin)-4,8-bis((2-ethylhexyl)-2,2'-bithiophene)-benzo[1,2-b:4,5-b′]dithiophene (BDTBT)[5] were synthesized according to previously reported synthetic methods.

Measurements

^1H and ^{13}C NMR spectra were recorded using a Varian Mercury Plus 300 MHz spectrometer, and the chemical shifts were recorded in units of ppm with chloroform as the internal standard. Elemental analysis was carried out using a Vario Micro Cube at the Korea Basic Science Institute (Busan, Korea). Absorption spectra were measured using a JASCO JP/V-570 model. The molecular weights of the polymers were determined by gel permeation chromatography (GPC) with polystyrene standards for calibration using a Waters high-pressure GPC assembly (model M590). Cyclic voltammetry (CV) was performed on a CH Instruments Electrochemical Analyzer. The CV measurements were carried out using acetonitrile containing 0.1 M tetrabutylammonium tetrafluoroborate ($TBABF_4$) as the supporting electrolyte and $Ag/AgNO_3$, platinum wire, and platinum as the reference, counter, and working electrodes, respectively.

Fabrication of Organic Thin-Film Transistors (OTFTs)

Organic thin-film transistors (OTFTs) were fabricated using a bottom-contact structure with a channel length (L) of 12 μm and width (W) of 120 μm. The source and drain contacts were composed of a 100 nm thick layer of gold, and the dielectric was 300 nm thick silicon dioxide (SiO_2). The SiO_2 surface was cleaned, dried, and pretreated with a 10.0 mM solution of octyltrichlorosilane (OTS-8) in toluene at room temperature for 2 h under a N_2 atmosphere to produce a non-polar and smooth surface onto which the polymers could be spin-coated. The polymers were dissolved in chlorobenzene at a concentration of 1.0 wt %. The solutions of organic semiconductors were spin-coated at 1000 rpm for 50 s to obtain thin films, which were annealed at 120 °C for 10 min. All device fabrication procedures and measurements were performed in air at room temperature.

Fabrication of Photovoltaic Devices

The devices fabricated in this study had an indium tin oxide (ITO)/PEDOT:PSS/polymer:$PC_{71}BM$/Ca/Al structure. ITO-coated glass substrates were consecutively cleaned by ultrasonication in detergent, distilled water, acetone, and 2-propanol. After ozone treatment of the cleaned ITO substrate for 20 min, a 40 nm–thick layer of PEDOT:PSS

(Clevios™ P VP AI4083) was spin-coated onto the surface. Then, the PEDOT:PSS layer was baked at 140 °C on a hot plate for 18 min. The polymer and $PC_{71}BM$ (100 nm) were layered by spin-coating using chlorobenzene with 3 vol % 1,8-diiodooctane as the solvent, which was filtered using a 0.45 μm syringe filter. Calcium (2 nm) and aluminum (120 nm) contacts were formed by vacuum deposition at pressures below 3×10^{-6} Torr, providing an active area of 9.0 mm^2. The thickness of the active layer was measured using a KLA Tencor Alpha-Step IQ surface profilometer with an accuracy of ±1 nm. The current density–voltage (J–V) characteristics of all the polymer photovoltaic cells were determined by illuminating the cells with simulated solar light (AM 1.5G) at an intensity of 100 mW/cm^2 using a K201 Lab50 solar simulator (McScience Inc.). Electrical data were recorded using a K101 Lab20 photovoltaic power meter (McScience Inc.) source-measure unit. The intensity of the simulated solar light was calibrated using a standard Si photodiode detector (K801S-K11; McScience Inc.), which was calibrated at the National Renewable Energy Laboratory (NREL). The external quantum efficiency (EQE) was measured as a function of wavelength in the range of 300–800 nm using a halogen lamp as the light source, and the calibration was performed using a Si reference photodiode. The measurements were performed after masking the entire fabricated device except the active cell area. All characterizations were carried out in an ambient laboratory atmosphere.

Synthesis

Synthesis of 5-(2-ethylhexylthio)-2,2'-bithiophene (1): n-Butyllithium (7.5 mL of 1.6 M solution in hexane, 12 mmol) was added dropwise into 2,2'-bithiophene (2.0 g, 12 mmol) and 50 mL of dry THF at 0 °C under a nitrogen atmosphere. After the mixture was stirred at 0 °C for 1.5 h, sulfur powder (0.38 g, 12 mmol) was added in one portion, and the resulting suspension was stirred at 0 °C for 2 h. Subsequently, 2-ethylhexylbromide (2.1 mL, 12 mmol) was added dropwise. The reaction mixture was stirred overnight at room temperature. Then, ice-water containing NH_4Cl was added to the reaction, and the mixture was extracted with ethyl acetate, washed with water, and dried over $MgSO_4$. After removal of the solvent, purification was carried out by silica gel column chromatography using hexane as the eluent. Compound **1** (2.2 g, 61% yield) was obtained as a colorless oil. ^{1}H NMR (300 MHz, $CDCl_3$, ppm): δ 7.20 (d, 1H), 7.13 (d, 1H), 7.00 (m, 3H), 2.83(d, 2H), 1.71–1.60 (q, 1H), 1.45–1.27 (q, 8H), 0.86 (m, 6H).

Synthesis of 4,8-bis((2-ethylhexylthio)-2,2'-bithiophene)benzo[1,2-b:4,5-b']dithiophene (2): Compound **1** (2.2 g, 7.3 mmol) and dry THF (50 mL) were added to a flask under a nitrogen atmosphere. The solution was cooled using an ice-water bath, and 5.1 mL of n-butyllithium (8.2 mmol, 1.6 M in hexane) was added dropwise; the solution was then stirred at room temperature for 1 h. Then, benzo[1,2-b:4,5-b']dithiophene-4,8-dione (0.4 g, 1.8 mmol) in THF (10 mL) was added, and the mixture was stirred for 2 h at 50 °C. After cooling to ambient temperature, $SnCl_2 \cdot 2H_2O$ (2.4 g, 10.9 mmol) in 10% HCl (5 mL) was added, and the mixture was stirred overnight. The resulting solution was poured into water and extracted with ethyl acetate. The organic layer was separated and dried using anhydrous $MgSO_4$. The obtained crude product was purified using silica-gel column chromatography with MC/HEX as the eluent. The desired product was crystallized as a yellow solid (0.64 g, 45% yield) from isopropyl alcohol (IPA). ^{1}H NMR (300 MHz, $CDCl_3$, ppm): δ 7.68 (d, 2H), 7.50 (d, 2H), 7.40 (d, 2H), 7.26 (d, 2H), 7.11 (d, 2H), 7.03 (d, 2H), 2.86 (d, 4H), 1.61–1.52 (m, 2H), 1.49–1.36 (m, 16H), 0.93–0.86 (m, 12H).

Synthesis of 2,6-bis(trimethyltin)-4,8-bis((2-ethylhexylthio)-2,2'-bithiophene)benzo[1,2-b:4,5-b']dithiophene (BDTBT-S) (3): Compound **2** (0.64 g, 0.8 mmol), N,N,N',N'-tetramethylethylenediamine (TMEDA) (0.2 g, 2.4 mmol), and THF (50 mL) were added to a flask under a nitrogen atmosphere. The solution was cooled to −78 °C, and 1.5 mL of n-butyllithium (2.4 mmol, 1.6 M in hexane) was added. The solution was stirred at −78 °C for 1 h, and then 2.4 mL of trimethyltin chloride (2.4 mmol, 1.0 M in THF) was added in one portion. The reaction mixture was stirred at room temperature for 2 h, and the cooling bath was then removed. The reaction mixture was stirred for 12 h. The resulting solution was poured into 50 mL of cold water and extracted three times with ethyl acetate. The organic layer was separated and dried using anhydrous $MgSO_4$. The solvent was removed under vacuum, and then the residue was crystallized from IPA. The desired product was obtained as a greenish yellow solid (0.4 g, 44% yield). ^{1}H NMR (300 MHz, $CDCl_3$, ppm): δ 7.69 (s, 2H), 7.40 (d, 2H), 7.28 (d, 2H), 7.12 (d, 2H), 7.03 (d, 2H), 2.86 (d, 4H), 1.72–1.54 (m, 2H), 1.50–1.30 (m, 16H), 0.93–0.86 (m, 12H), 0.41 (s, 18H). ^{13}C NMR (75 MHz, $CDCl_3$, ppm): δ 143.40, 143.15, 139.86, 139.34, 137.83, 137.44, 135.41, 133.50, 130.84, 128.94, 127.91, 123.98, 121.82, 43.62, 38.91, 31.96, 28.81, 25.22, 22.98, 14.22, 10.64, −8.20.

General Polymerization Procedure

The two copolymers were synthesized using Stille-coupling polymerization, as shown in *Scheme* 2. 2,6-Bis(trimethyltin)-4,8-bis((2-ethylhexyl)-2,2'bithiophene)benzo[1,2-

b:4,5-b′]dithiophene (BDTBT), 2,6-bis(trimethyltin)-4,8-bis((2-ethylhexylthio)-2,2'-bithiophene)benzo[1,2-b:4,5-b′]dithiophene (BDTBT-S), and 4,7-bis(5-bromo-4-(2-ethylhexyl)-2-thiophene)-2,1,3-benzothiadiazole (DTBT) were synthesized using previously reported procedures.[12,16] Tetrakis(triphenylphosphine)palladium in 5 mL of anhydrous toluene and 1 mL of DMF was stirred at 110 °C overnight. Excess 2-bromothiophene and tripropyl(thiophen-2-yl)stannane (as the end-capper) dissolved in 1 mL of anhydrous toluene was added, and the mixture was stirred for 12 h. The reaction mixture was cooled to approximately 50 °C, and 200 mL of methanol was added slowly with vigorous stirring. The polymer fibers were collected by filtration and re-precipitated from methanol and acetone. The polymers were then purified further by washing them for one day with acetone in a Soxhlet apparatus to remove the oligomers and catalyst residues. The polymers were then subjected to column chromatography with chloroform, and the polymers were re-precipitated from a chloroform/methanol mixture several times. The resulting polymers were soluble in common organic solvents.

Synthesis of PBDTBT-DTBT

BDTBT (300 mg, 0.3 mmol) was mixed with DTBT (192 mg, 0.3 mmol), tetrakis(triphenylphosphine)palladium (16 mg, 2.6 μmol), toluene (5 mL), and DMF (1 mL). The polymer yield was 13% (M_n = 5000 , PDI = 1.3). Anal. Calcd for $C_{72}H_{82}N_2S_9$: C, 68.41; H,6.54; N, 2.22, Found: C, 68.10; H, 6.66. N, 2.01.

Synthesis of PBDTBT-S-DTBT

BDTBT-S (300 mg, 0.3 mmol) was mixed with DTBT (181 mg, 0.3 mmol), tetrakis(triphenylphosphine)palladium (16 mg, 2.6 μmol), toluene (5 mL), and DMF (1 mL). The polymer yield was 18% (M_n = 5300 , PDI = 1.6). Anal. Calcd for $C_{72}H_{82}N_2S_{11}$: C, 65.11; H,6.22; N, 2.11, Found: C, 64.97; H, 6.31. N, 1.98.

RESULTS AND DISCUSSION

Synthesis and Characterization

The synthetic routes for the monomers and polymers are outlined in *Schemes* 1 and 2, respectively. ^{1}H NMR spectra of the newly synthesized 2,6-bis(trimethyltin)-4,8-bis((2-ethylhexyl)-2,2'-bithiophene)-benzo[1,2-b:4,5-b']dithiophene (BDTBT) and 2,6-bis(trimethyltin)-4,8-bis((2-ethylhexylthio)-2,2'-bithiophene)benzo[1,2-b:4,5-b′]dithiophene (BDTBT-S) were shown in *Figure* 1(a) and (b). Polymerization was carried out with $Pd(PPh_3)_4$ as the catalyst, and the reaction was refluxed for 16 h under an argon atmosphere. The obtained crude polymers were purified by successive extractions with methanol, hexane, acetone, and chloroform. The synthesized polymers possessed good solubility in chloroform (CF), chlorobenzene (CB), and o-dichlorobenzene (o-DCB). PBDTBT-DTBT and PBDTBT-S-DTBT based on the BDT unit with 2,2'-bithiophene were found to be only sparingly soluble in chloroform possibly because of the enhanced intermolecular interactions caused by the introduction of the bithiophene moiety with extended conjugation. The soluble fraction of the polymers obtained using a Soxhlet extractor showed a relatively low average molecular weight.[17] The molecular weight and polydispersity index (PDI) were determined by GPC calibrated against polystyrene standards in a chloroform eluent at room temperature. The number average molecular weights (M_n) of PBDTBT-DTBT and PBDTBT-S-DTBT were 5000 and 5300 g/mol with PDIs of 1.3 and 1.6, respectively.

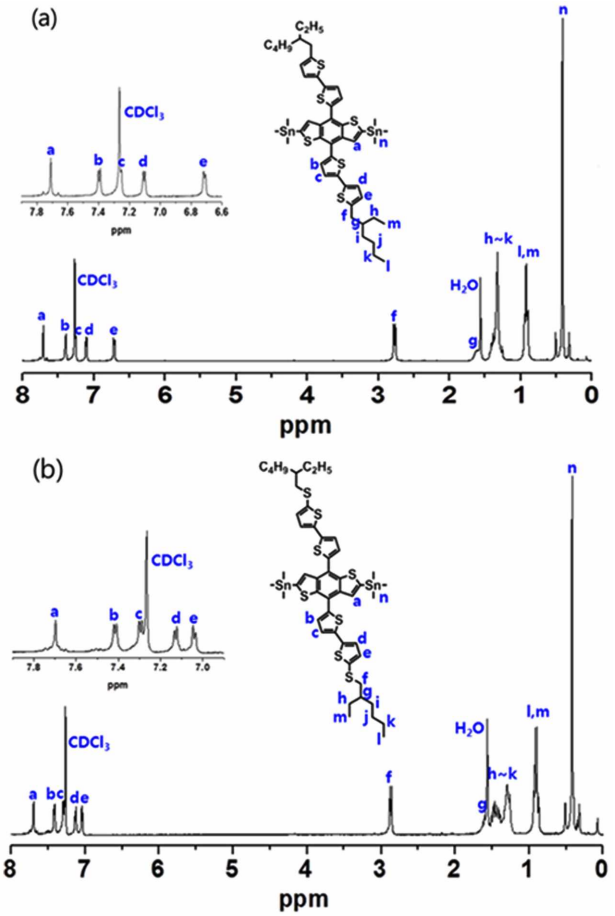

***Figure* 1.** (a) ^{1}H NMR spectra of 2,6-bis(trimethyltin)-4,8-bis((2-ethylhexyl)-2,2'-bithiophene)-benzo[1,2-b:4,5-b']dithiophene (BDTBT) and (b) 2,6-bis(trimethyltin)-4,8-bis((2-ethylhexylthio)-2,2'-bithiophene)benzo[1,2-b:4,5-b']dithiophene (BDTBT-S) in $CDCl_3$.

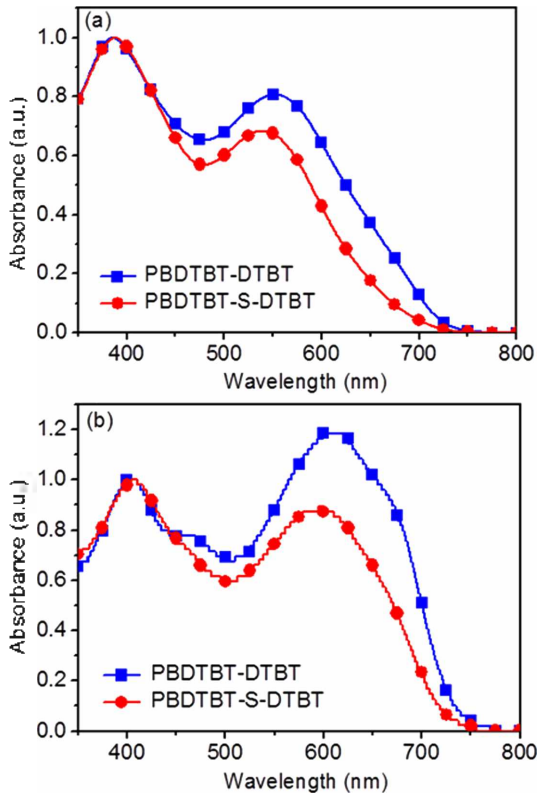

***Figure* 2.** Normalized UV–visible absorption spectra of the polymers (a) in chloroform solution and (b) as thin films.

Optical and Electrochemical Properties

The UV-visible absorption spectra of PBDTBT-DTBT and PBDTBT-S-DTBT in dilute chloroform solutions and thin films are shown in *Figure* 2. In the solution state, the polymers showed two broad and strong absorption bands at around 390 and 550 nm. The absorption band observed at the shorter wavelength is due to a π–π* transition of the polymer backbone, and the band at the longer wavelength region was attributed to intramolecular charge transfer (ICT) between the donor and acceptor units. The absorption bands of the polymers were more red-shifted in the film state than those of the corresponding polymer solutions. The red shift is caused by the increased inter-chain π-π interaction between the polymer chains in the film. Moreover, the absorptions at the longer wavelength region were much more intense in the film state, implying that the ICT of the polymer films was stronger than that in the solution state.[18] The optical band-gap energies (E_g^{opt}) of the polymers were determined from the UV-visible absorption onset. The absorption onsets for PBDTBT-DTBT and PBDTBT-S-DTBT were 731 and 721 nm, respectively, and, consequently, the optical band gaps of PBDTBT-DTBT and PBDTBT-S-DTBT were 1.69 and 1.72 eV, respectively.

To determine the HOMO energy levels of the polymers, we performed CV using a Ag/Ag+ electrode as a reference electrode and the redox potential of ferrocene/ferrocenium (Fc/Fc−) as a calibrated standard. The redox potential of Fc/Fc· has an absolute energy level of 4.80 eV in a vacuum. In this external standard under the same conditions, the potential was 0.086 eV; therefore, the following equation was defined: $E_{HOMO} = -(E_{ox}^{onset} + 4.714)$ eV. The measured onset oxidation potentials (E_{ox}^{onset}) for PBDTBT-DTBT and PBDTBT-S-DTBT were 0.61 and 0.69 eV, respectively, which correspond to HOMO energy levels of 5.32 and 5.40 eV, respectively. The HOMO energy level of PBDTBT-S-DTBT was ~0.08 eV lower than that of PBDTBT-DTBT indicating that the alkylthio side-chains in the copolymer could significantly influence the electronic properties of the polymer. This trend is in agreement with earlier studies that reported that the introduction of alkylthio substituents results in lower HOMO levels because of the π-acceptor ability of sulfur atoms.[9,19]

The d-orbital of the sulfur atom in the alkylthio group accepts π-electrons from the p-orbital of the adjacent thiophene ring, which enables the alkylthio substituent to lower the energy levels of the HOMO/LUMO frontier orbitals. Meanwhile, the LUMO levels of the polymers were determined by combining the HOMO levels obtained fromthe CV measurements with the E_g^{opt} values obtained from the UV-visible absorption edges. Accordingly, the LUMO energy levels of PBDTBT-DTBT and PBDTBT-S-DTBT were estimated to be −3.63 and −3.68 eV, respectively. The LUMO energy levels of the polymers were within a suitable range and were higher than that of $PC_{71}BM$ (ca. −4.30 eV); thus, efficient exciton dissociation would be expected in OPV devices containing these polymers.[20] The UV-visible absorption properties, E_g^{opt} values, and HOMO/LUMO energy levels of the polymers are summarized in *Table* 1.

***Table* 1.** Optical and electrochemical properties of the synthesized polymers

polymer	λ_{max} (nm)		λ_{edge}	E_g^{opt}	HOMO	LUMO
	solution[a]	film[b]	(nm)	(eV)	(eV)	(eV)
PBDTBT-DTBT	546	604	731	1.69	-5.32	-3.63
PBDTBT-S-DTBT	541	591	721	1.72	-5.40	-3.68

[a]Measured in dilute CF solutions. [b]Measured on quartz plates containing the corresponding spun-cast films.

Density Functional Theory (DFT) Calculations

To investigate the effect of the sulfur atom on the side-chain of the polymer, we performed DFT calculations using B3LYP functional and 6-31G(d) basis sets. We calculated the dimer compounds using D–A–D–A structured models, i.e., BDTBT–DTBT–BDTBT–DTBT and BDTBT-S–DTBT–BDTBT-S–DTBT. To simplify the calculations, we used a shorter iso-butyl group instead of the 2-ethylhexyl group as a side-chain in both the BDT and DTBT units. The structures of the model compounds calculated by DFT are shown in *Figures* 3(a) and (b), which also show the energy levels and electron distributions of the HOMO and LUMO frontier orbitals of BDTBT–DTBT–BDTBT–DTBT and BDTBT-S–DTBT–BDTBT-S–DTBT. The electrons in the HOMO for all the model compounds were delocalized along the dimer backbone; in contrast, in the LUMO, they were mainly localized in the accepting unit, i.e., DTBT. This explains why the model compounds with electron donating accepting structures had intense ICT. The HOMO and LUMO energy levels of the BDTBT-S-DTBT dimer were lower than those of the BDTBT-DTBT dimer, and the band gap of the BDTBT-S-DTBT dimer was slightly larger than that of the BDTBT-DTBT dimer. These results are consistent with the optical band gaps and HOMO energy levels of the polymers determined via UV-visible absorption and CV measurements, respectively. The dihedral angles between the BDT and DTBT units were also calculated. The dihedral angles of the BDTBT–DTBT and BDTBT-S–DTBT dimers are summarized in *Table* 2.

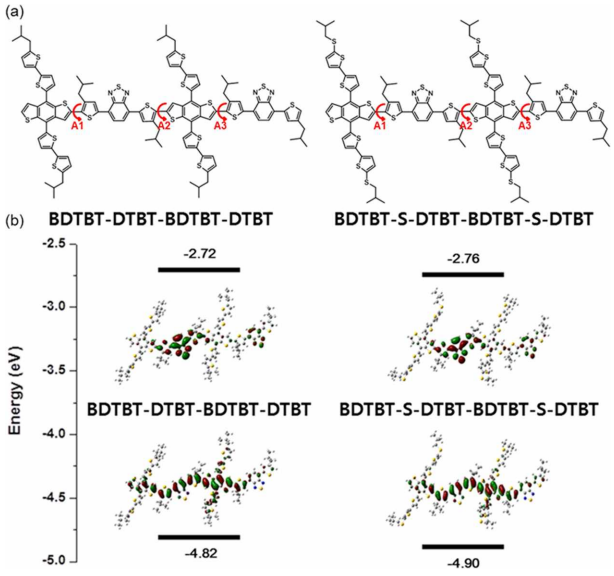

***Figure* 3.** (a) Chemical structures and (b) energy levels and electron distributions of the HOMO and LUMO frontier orbitals of the model compounds obtained from DFT calculations.

***Table* 2.** Dihedral angles of the model compounds with a D–A–D–A structure, as calculated by DFT

Polymer	Dihedral Angle (°)		
	A1	A2	A3
PBDTBT-DTBT	33.0	33.2	42.6
PBDTBT-S-DTBT	30.9	31.9	36.3

In the BDTBT-DTBT dimer structure, the A1, A2, and A3 dihedral angles were 33.0 °, 33.2 °, and 42.6 °, respectively. The corresponding dihedral angles of the BDTBT-S-DTBT dimer were 30.9 °, 31.9 °, and 36.3 °, respectively. These results suggest that BDTBT-S–DTBT–BDTBT-S–DTBT had a more planar structure than BDTBT–DTBT–BDTBT–DTBT. The more planar BDTBT-S–DTBT dimer could be expected to have higher charge carrier mobility than the BDTBT–DTBT dimer.

Organic Thin-Film Transistor Characteristics

We fabricated OTFTs to measure the field-effect charge mobilities of the polymers. The fabricated OTFTs had bottom-contact geometries (channel length of 12 μm and width of 120 μm) on silicon wafers. *Figure* 4 shows the transfer curves of devices using PBDTBT-DTBT and PBDTBT-S-DTBT as the active layers. The fabricated OTFTs exhibited typical p-type transistor behavior. In the saturation regime, the mobilities were calculated using the following equation: $I_{ds} = (WC_i/2L)\mu(V_{gs}-V_{th})^2$, where I_{ds} is the drain-source current, L is the channel length, W is the channel width, C_i is the capacitance per unit area of the insulating layer, V_{gs} is the gate voltage, V_{th} is the threshold voltage, and μ is the field-effect mobility.[21] The OTFTs fabricated using PBDTBT-S-DTBT showed a hole mobility of 5.8×10^{-4} $cm^2/V{\cdot}s$, which was higher than the 5.3×10^{-5} $cm^2/V{\cdot}s$ obtained for the device fabricated using PBDTBT-DTBT. The higher hole mobility of PBDTBT-S-DTBT than PBDTBT-DTBT would be attributed to the stronger inter-polymer chain interactions in PBDTBT-S-DTBT induced by the alkylthio substituted on the bithiophene conjugated side chains.

Performance of Bulk Heterojunction (BHJ) OPVs

To test the photovoltaic performances of PBDTBT-DTBT and PBDTBT-S-DTBT, we fabricated OPV devices using the polymers as p-type donors and $PC_{71}BM$ as the electron acceptor with a device configuration of ITO/PEDOT:PSS/polymer:$PC_{71}BM$/Ca/Al. The active layers were spin-coated from a solution of the donor polymer and acceptor in chlorobenzene. The donor-to-acceptor composition ratio of the active layers was adjusted from 1.0 : 1.0 to 1.0 : 2.0 (w/w) for optimization. The fabricated devices showed the high-

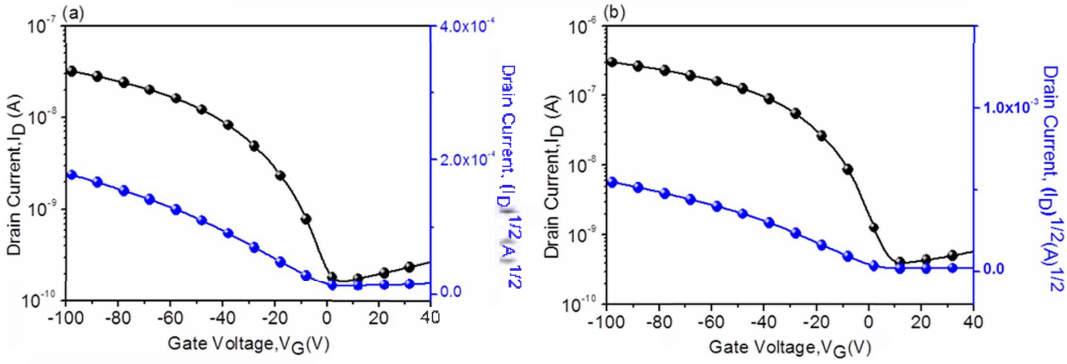

***Figure* 4.** Transfer characteristics of OTFTs fabricated using the polymers as the active layers at a constant source–drain voltage of −60 V: (a) PBDTBT-DTBT and (b) PBDTBT-S-DTBT.

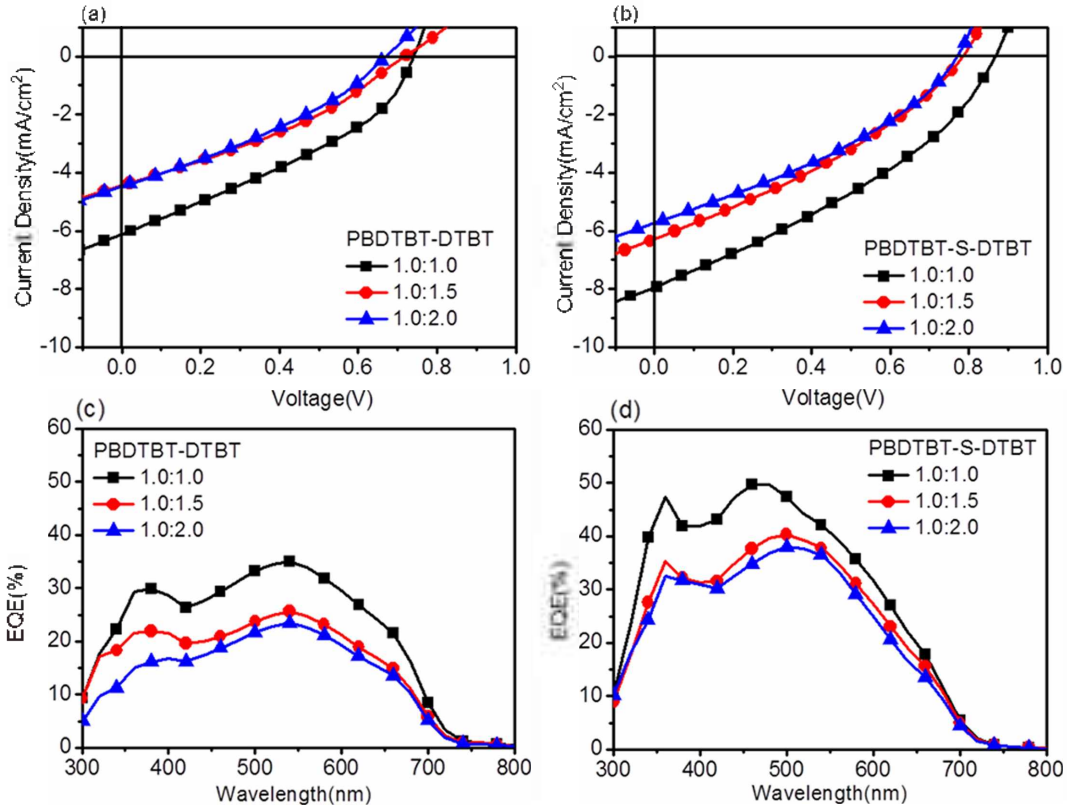

***Figure* 5.** J–V curves and EQE curves of solar cell devices with (a and c) PBDTBT-DTBT/$PC_{71}BM$ (w/w) and (b and d) PBDTBT-S-DTBT/$PC_{71}BM$ (w/w) under AM 1.5G illumination (100 mW/cm^2).

est short-circuit currents (J_{sc}) at a donor-to-acceptor composition ratio of 1.0 : 1.0. 1,8-Diiodooctane (DIO, 3 vol %) was used as a processing additive to optimize the morphology of the p-n heterojunction in the active layer.

Figures 5(a) and (b) show J–V curves of the OPVs. The highest PCE values of the devices fabricated using PBDTBT-DTBT and PBDTBT-S-DTBT were 1.59% and 2.05%, respectively. The open-circuit voltages (V_{OC}) were 0.74 and 0.83 V for the PBDTBT-DTBT and PBDTBT-S-DTBT devices, respectively. It is well-known that the V_{OC} is proportional to the energy gap between the HOMO energy level of the donor polymer and LUMO energy level of the acceptor. The V_{OC} value of the OPV based on PBDTBT-S-DTBT is 0.08 V higher than that of the OPV based on PBDTBT-DTBT, which is consistent with the lower HOMO energy levels of the alkylthio side-chains containing PBDTBT-S-DTBT. The measured J_{SC} values of PBDTBT-DTBT and PBDTBT-S-DTBT were 6.12 and 7.56 mA/cm^2, respectively, in their optimized PCE devices. The higher hole mobility of the alkylthio side-chain–containing polymer (PBDTBT-S-DTBT)

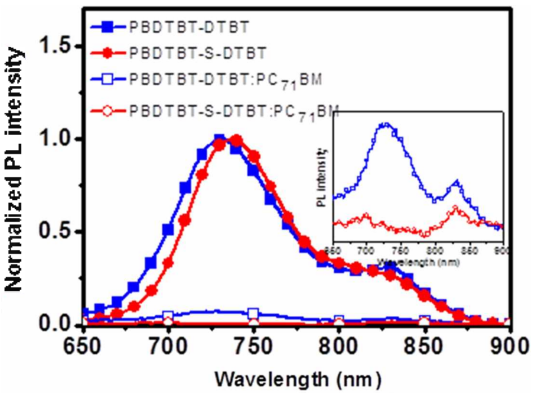

***Figure* 6.** Photoluminescence spectra of PBDTBT-DTBT, PBDTBT-DTBT:$PC_{71}BM$, PBDTBT-S-DTBT, and PBDTBT-S-DTBT:$PC_{71}BM$ films.

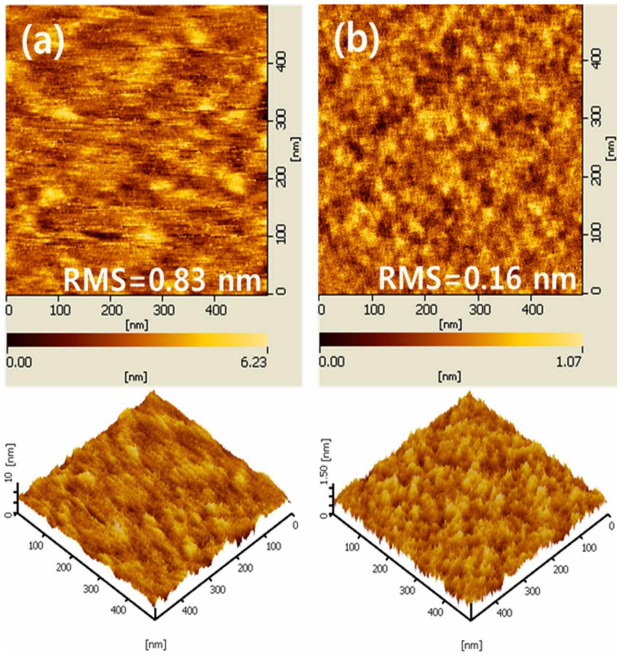

***Figure* 7.** AFM images obtained in the tapping-mode of the surface of (a) PBDTBT-DTBT:$PC_{71}BM$ (1:1 wt %) and (b) PBDTBT-S-DTBT:$PC_{71}BM$ (1:1 wt %) thin films spin-coated from CB/3 vol % DIO.

was consistent with their higher J_{SC} values, as compared to those of the corresponding devices using PBDTBT-DTBT. In OPV devices, the photoluminescence (PL) quenching effect is an important parameter of donor materials to ensure efficient charge-carrier transport to the electrodes and suppress photocurrent loss by competing charge recombination.[22] We measured the PL quenching of the pure polymer and blended active films under optimized conditions in the OPVs.

Figure 6 shows that PBDTBT-DTBT and PBDTBT-S-DTBT had PL emission bands with emission maxima at 731 and 737 nm, respectively. The emission band for PBDTBT-S-DTBT in the polymer:$PC_{71}BM$ blend was more effectively quenched than that of PBDTBT-DTBT; this suggests that PBDTBT-S-DTBT in an OPV formed a larger number of free charges with a concurrent increase in the photocurrent.

To investigate the p-n heterojunction morphology, an atomic force microscopy (AFM) was employed for the donor-acceptor blend films (1.0 : 1.0, w/w, 3 vol % DIO). As shown in *Figure* 7, the blend films based on PBDTBT-DTBT:$PC_{71}BM$ and PBDTBT-S-DTBT:$PC_{71}BM$ exhibited uniform and bi-continuous networks, indicating good miscibility between the polymer donor and $PC_{71}BM$. The interpenetrating network between polymers and $PC_{71}BM$ provides a large interfacial area for efficient charge separation and transportation to achieve high J_{SC} and FF in their OPVs. The PBDTBT-S-DTBT film showed a smoother surface than the PBDTBT-DTBT film. The root mean square (RMS) roughness of PBDTBT-DTBT and PBDTBT-S-DTBT:$PC_{71}BM$ blend films were 0.83 and 0.26 nm, respectively.

To verify the accuracy of the photo J–V measurements, the corresponding external quantum efficiency (EQE) spectra of the devices described above were measured under illumination with monochromatic light, as shown in *Figures* 5(c) and (d).

Compared to the absorption spectra of the pristine poly-

***Table* 3.** Photovoltaic properties of OPVs with an ITO/PEDOT: PSS/polymers:$PC_{71}BM$/Ca/Al inverted structure under AM 1.5G (100 mW/cm^2) illumination

polymer	ratio [w/w]	V_{OC} [V][a]	J_{SC} [mA/cm^2][a]	FF [%][a]	PCE [%][a]
PBDTBT-DTBT	1.0 : 1.0	0.74	6.12	35	1.59
	1:0 : 1.5	0.72	4.45	32	1.05
	1.0 : 2.0	0.71	4.00	33	0.96
PBDTBT-S-DTBT	1.0 : 1.0	0.83	7.56	33	2.05
	1:0 : 1.5	0.78	6.29	33	1.61
	1.0 : 2.0	0.77	5.74	34	1.51

[a]Photovoltaic properties of polymer:$PC_{71}BM$ based devices spin-coated from a chlorobenzene with 1,8-diiodooctane 3 vol % solution for polymers.

mers, the substantially broader EQE responses in the visible region were attributed to the intrinsic absorption of both the polymers and $PC_{71}BM$. The integrated J_{SC} values from the EQE spectra were 5.95 and 7.27 mA/cm^2 for PBDTBT-DTBT and PBDTBT-S-DTBT, respectively. The J_{SC} values calculated from integration of the EQE spectra are within a 5% error, which correlates well with those obtained from the J–V measurements, thereby supporting the reliability of the photovoltaic measurements. The photovoltaic parameters of the optimized devices are summarized in *Table* 3.

CONCLUSION

In conclusion, we synthesized a new 2D-conjugated polymer, PBDTBT-S-DTBT, based on BDT with 5-(2-ethylhexylthio)-2,2'-bithiophene as the donor unit and DTBT as the acceptor unit. We analyzed the properties of the polymer with respect to those of PBDTBT-DTBT. The results indicated that molecular modification by introducing an alkylthio group onto the conjugated thieno[3,2-b]thiophene side-chain is a promising strategy to lower the HOMO energy level and increase the hole mobilities of the donor polymers to improve the OPV performance.

Acknowledgments. This work was supported by a 2-Year Research Grant of Pusan National University.

REFERENCES

1. Li, G.; Zhu, R.; Yang, Y. *Nat. Photonics* **2012**, *6*, 153.
2. Dou, L.; You, J.; Yang, J.; Chen, C.-C.; He, Y.; Murase, S.; Moriaty, T.; Emery, K.; Li, G; Yang, Y. *Nat. Photonics* **2012**, *6*, 180.
3. Zhang, M.; Guo, X.; Zhang, S.; Hou, J. *Adv. Mater.* **2014**, *26*, 1118.
4. Baek, M.-J.; Lee, S.-H.; Kim, D. H.; Lee, Y.-S. *Macromol. Res.* **2012**, *20*, 147.
5. Kim, J.-H.; Song, C. E.; Kim, H. U.; Kang, I.-N.; Shin, W. S.; Park, M.-J.; Hwang, D.-H. *J. Polym. Sci. Pol. Chem.* **2013**, *51*, 4136.
6. Chen, H.-Y.; Hou, J.; Zhang, S.; Liang, Y.; Yang, G; Yang, Y.; Yu, L.; Wu, Y.; Li, G; *Nat. Photonics* **2009**, *3*, 649.
7. Zhou, H.; Yang, L.; Stuart, A. C.; Price, S. C.; Liu, S.; You, W. *Angew. Chem. Int. Edit* **2011**, *50*, 2995.
8. Cui, C.; Wong, W.-Y.; Li, Y. *Energ. Environ. Sci.* **2014**, *7*, 2276.
9. Ye, L.; Zhang, S.; Zhao, W.; Yao, H.; Hou, J. *Chem. Mater.* **2014**, *26*, 3603.
10. Kim, J.-H.; Park, J.B.; Jung, I.H.; Yoon, S.C.; Kwak, J.; Hwang, D.-H.; *J. Mater. Chem. C* **2015**, *3*, 4250.
11. Brabec, C. J.; Cravino, A.; Meissner, D.; Sariciftci, N. S.; Fromherz, T.; Rispens, M. T.; Sanchez, L.; Hummelen, J. C.; *Adv.Funct. Mater.* **2001**, *11*, 374.
12. Wang, N.; Chen, Z.; Wei, W.; Jiang, Z.; *J. Am. Chem. Soc.* **2013**, *135*, 17060.
13. Lee, J.; Kim, M.; Kang, B.; Jo, S. B.; Kim, H. G; Shin, J.; Cho, K.; *Adv. Energy Mater.* **2014**, *4*, 1400087.
14. Fang, K.; Huang, W.; Chang, G.; Yang, J.; Shen, Y.; Ye, X.; *Macromol. Res.* **2015**, *23*, 545.
15. Cui, C.; Wong, W.-Y.; Li, Y.; *Energy Environ. Sci.* **2014**, *7*, 2276.
16. Hou, Q.; Zhou, Q.; Zhang, Y.; Yang, W.; Yang, R.; Cao, Y. *Macromolecules* **2004**, *37*, 6299.
17. Hong, W.; Guo, C.; Li, Y.; Zheng, Y.; Huang, C.; Lu, S.; Facchetti, A. *J. Mater. Chem.* **2012**, *22*, 22282.
18. Kim, J.-H.; Shin, S. A.; Park, J. B.; Song, C. E.; Shin, W. S.; Yang, H.; Li, Y.; Hwang, D.-H. *Macromolecules* **2014**, *47*, 1613.
19. Lee, D.; Stone, S. W.; Ferraris, J. P. *Chem. Comm.* **2011**, *47*, 10987.
20. Thompson, B. C.; Fréchet, J. M. J. *Angew. Chem. Int. Edit* **2008**, *47*, 58.
21. Dimitrakopoulos, C. D.; Malenfant, P. R. L. *Adv. Mater.* **2002**, *14*, 99.
22. Kim, K. H.; Kim, D. C.; Cho, M. J.; Choi, D. H. *Macromol. Res.* **2009**, *17*, 549.